

CAVITATION EROSION OF WELDED MARTENSITIC STAINLESS STEEL COATINGS¹

Julián David Escobar Atehortúa²
Ricardo Correa Colorado³
Juan Felipe Santa Marín⁴
Jorge Enrique Giraldo Barrada⁵
Alejandro Toro⁶

Abstract

Cavitation is an issue in hydro-electric plants. Many turbines are made in 13Cr-4Ni stainless steel and must be repaired by welding in the field under very narrow time-frames. In this paper, the cavitation erosion resistance of welded martensitic stainless steels applied by semi-automatic process with a high deposition rate was tested in laboratory. The coatings were applied by GMAW transfer process using pulsed (GMAW-P) and non-pulsed (GMAW-S) welding current, a constant voltage power supply, and an AWS A5.9 ER410NiMo filler metal (1.2mm diameter) under argon-based shielding gas. The cavitation erosion tests were done in a vibratory apparatus according to ASTM G32 standard. The incubation period, the maximum erosion rate and the variation of surface roughness during the tests were reported and the results were compared with those obtained for uncoated 13Cr-4Ni steel. Cavitation erosion resistance of GMAW-P coatings was higher than that of the substrate and GMAW-S coatings. After a reference time of 8 hours of testing, the cumulative mass loss of GMAW-P coating (3.93mg) was 3 and 2 times lower than that of reference materials GMAW-S (11.49mg) and 13Cr-4Ni steel (7.8mg), respectively. The maximum erosion rate of GMAW-P coatings (1.14 mgh^{-1}) was lower than the 13Cr-4Ni substrate (2.01 mgh^{-1}) and GMAW-S coatings (1.54 mgh^{-1}). The incubation period of the coatings showed the highest value for GMAW-P coatings (5h) with a 33% of improvement with respect to 13Cr-4Ni substrate (3.75h).

Key words: Cavitation erosion; Incubation period; Pulsed GMAW coatings; Roughness parameters.

EROSÃO POR CAVITAÇÃO DE REVESTIMENTOS SOLDADOS DE AÇO INOXIDÁVEL MARTENSÍTICO

Resumo

Cavitação é um problema em usinas hidrelétricas. Muitas turbinas são feitas em aço inoxidável 13Cr-4Ni que devem ser reparadas por soldagem no lugar de trabalho sob grandes restrições de tempo, pois nas usinas a disponibilidade é o indicador mais importante. Neste trabalho, a resistência à cavitação de aços inoxidáveis martensíticos soldados utilizando uma elevada taxa de deposição mediante processo semi-automático foi testada em laboratório, a fim de decidir se os depósitos obtidos são uma boa opção para recuperação de turbinas desgastadas. Os revestimentos foram aplicados por um processo de transferência pulsado usando uma fonte de tensão constante, sob atmosfera de argônio e utilizando um metal de aporte ER410NiMo (1.2 mm de diâmetro) de acordo com a especificação AWS A5.4. Os testes de cavitação foram realizados em um cavitômetro vibratório de acordo com a norma ASTM G32. O período de incubação, a taxa de erosão máxima e a variação da rugosidade da superfície foram medidos durante as provas e os resultados foram comparados com os obtidos para o aço 13Cr-4Ni sem revestir. Os resultados mostraram que a resistência à cavitação dos revestimentos GMAW-P foi superior à do aço não revestido e do revestimento GMAW-S. Depois de um tempo de prova de referência de 8 horas, a perda de massa acumulada do revestimento GMAW-P (3.93 mg) foi de 3 e 2 vezes menor que a dos materiais de referência GMAW-S (11.49 mg) e 13Cr-4Ni aço (7.8 mg), respectivamente. A taxa de erosão máxima dos revestimentos GMAW-P (1.14 mgh^{-1}) foi menor do que a do substrato 13Cr-4Ni (2.01 mgh^{-1}) e os revestimentos GMAW-S (1.54 mgh^{-1}). O período de incubação dos revestimentos, usando o valor médio de dois critérios de cálculo, apresentou o maior valor para os revestimentos GMAW-P (5h), com 33% de melhoria com relação ao substrato 13Cr-4Ni (3.75h).

Palavras-chave: Cavitação; GMAW pulsado; Parâmetros de rugosidade; Período de incubação.

¹ Technical contribution to the First International Brazilian Conference on Tribology – TribobR-2010, November, 24th-26th, 2010, Rio de Janeiro, RJ, Brazil.

² Welding Laboratory, Tribology and surfaces laboratory. National University of Colombia, Medellín. juliandesobar@gmail.com

³ Welding Laboratory, Tribology and surfaces laboratory. National University of Colombia, Medellín. rjchi.1@gmail.com

⁴ Welding Laboratory, Tribology and surfaces laboratory. National University of Colombia, Medellín. jfsanta@unal.com

⁵ Tribology and surfaces laboratory. National University of Colombia, Medellín. jegirald@unal.edu.co

⁶ Welding Laboratory. National University of Colombia, Medellín. aotoro@unal.edu.co

1 INTRODUCTION

Worn Pelton and Francis turbines are usually repaired by welding to ensure proper operation. Traditionally, welding repairs have been carried out by using Shielded Metal Arc Welding (SMAW) process. However, SMAW process has some limitations such as low deposition rates and higher hydrogen contents compared with Gas Metal Arc Welding (GMAW) process.^(1,2) GMAW process uses a continuous electrode (increasing deposition rates) and both welding current and voltage can be controlled to obtain different metal transfer modes.^(3,4) One of the latest developments in GMAW process is pulsed transfer mode. In this mode, the heat input is reduced by changing a constant value of current for a waved one where the maximum and minimum values of current and the time for each one are controlled.⁽⁵⁾ The mechanical properties of this process have been broadly studied but few researchers have reported the wear resistance obtained under specific conditions.

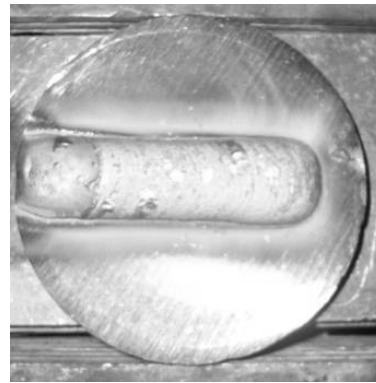
In this work the cavitation erosion of welded martensitic stainless steels coatings was studied. The applied coatings are potential solutions to repair worn turbines or mechanical components in hydropower plants and they were obtained using two different transfer modes in order to compare their effect on cavitation erosion resistance. The study focused on the wear mechanisms of the coating that showed the best behavior in order to evaluate the evolution of the morphology of the surfaces during cavitation erosion tests.

2 EXPERIMENTAL PROCEDURE

2.1 Experimental Setup

Cavitation erosion resistance of martensitic stainless steel coatings applied on ASTM A743 grade CA6NM steel plates (from now on, 13Cr-4Ni steel) with 12.7mm in thickness was tested. The coated samples, which will be referred to as GMAW-P and GMAW-S from this point on, were obtained after applying GMAW process by using Spray and Pulsed metal transfer modes respectively, in the 1-G plane position for not overlapped bead-on-plate welding condition.

Figure 1 shows the experimental setup designed to ensure the same welding conditions for traveling speed, nozzle-work piece distance, welding gun angle amplitude and frequency parameters for each coating. Welding of coatings and joints were performed using a MILLER-Invision 456MP constant voltage welding equipment for direct and pulsed current and a BUG-O modular system with a MDS-1005 control to mechanize welding application. Table 1 shows the welding parameters for GMAW-P and GMAW-S coatings. The 13Cr-4Ni steel (used as reference material) was received in the as-cast condition and it was homogenized at 1050°C for 1 h and then air-cooled to room temperature. After that, the steel specimens were tempered at 620 °C for 1h and cooled down in air.



a) Experimental setup
b) Bead-on-plate
Figure 1. Experimental setup for joint and bead on plate testing.

2.2 Materials

The coatings were applied using an AWS A5.9 ER 410 NiMo filler metal electrode with 1.2mm in diameter. This solid wire is widely used in hydropower industry for repairing worn surfaces of hydraulic components. The atmosphere was shielded with 98 % Ar - 2 % O₂ in both metal transfer modes using a gas flow of 15 l/min, a 12.7 mm diameter gas nozzle, and 20mm nozzle-to-work piece distance.

Table 1. Welding parameters

Essential Variables	GMAW-P	GMAW-S
Welding speed (m/min)	0.09	0.1651
Wire feed speed (m/min)	7.3	7,4
Voltage (V)	31	33
Current (A)	183	255
Pre-heating temperature (°C)	150	150
Amplitude (mm)	35	N.A.
Frequency (1/min)	30	N.A.
Peak current / base (A)	402 / 103	N.A.
Peak time / base (s x E-3)	1.85 / 5.1	N.A.
Trim / Frequency	30 / 145/s	N.A.
Average Current (A)	183	N.A.
Mode	No adaptive	N.A.

The nominal and measured chemical compositions of the stainless steel and the welded coatings obtained for the samples are shown in **table 2**. Chemical composition of the coatings was obtained using Optical Emission Spectrometry technique in a Shimadzu OES 5500.

Table 2. Chemical composition of tested samples, measured by Optical Emission Spectrometry

Material	C	Mn	Si	P	S	Cr	Ni	Mo	Fe
ASTM A743 grade CA6NM (13Cr-4Ni)	0.06	1.00	1.00	0.04	0.03	11.5-14.00	3.2-4.5	0.4-1	Balance
AWS A5.9 ER410NiMo	0.06	0.6	0.5	0.03	0.03	11.0-12.5	4.0-5.0	0.4-0.7	Balance
GMAW-S	0.033	0.726	0.489	0.021	0.004	12.55	4.49	0.558	Balance
GMAW-P	0.024	0.363	0.352	0.012	0.003	12.577	5.161	0.456	Balance

2.3 Microstructure Characterization

The microstructure of the coatings was analyzed by a Light Optical Microscopy (LOM) using a Nikon Eclipse LV100 microscope with a Nikon Digital Sight DS-2Mv camera and a Scanning Electron Microscopy (SEM) JEOL 5910LV. 3D-reconstructions of worn surfaces were performed every hour by processing images taken under different focusing conditions with the aid of NIS-Elements software.

2.4 Cavitation Erosion Tests

Cavitation erosion tests were carried out in ultrasonic equipment according to ASTM G32 standard. Test samples(see Figure 2 for details) were held stationary below a vibrating horn at a distance of $0.5 \pm 0.02 \text{ mm}$ (unattached method). The frequency of vibration and the peak-to-peak displacement amplitude of the horn were $20 \pm 0.5 \text{ KHz}$ and $50 \mu\text{m}$, respectively, and the test liquid was distilled water maintained at $25 \pm 0.5^\circ\text{C}$.

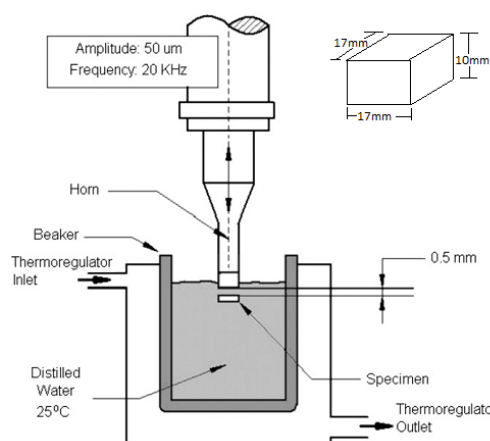


Figure 2. Ultrasonic equipment for cavitation erosion tests

Prior to the tests, all the samples were polished on emery papers ASTM 80, 240, 320, 400 and 600 in order to obtain surfaces with mean squared roughness (R_q) lower than $1 \mu\text{m}$. Cavitation erosion tests lasted between 8h and 14h, being the mass losses and the roughness changes monitored every hour. After the tests, the worn surfaces were analyzed by SEM in order to identify the main wear mechanisms. The cavitation erosion resistance was discussed in terms of the measured mass losses and the topographical features of the worn surfaces.

2.5 Surface Topography Measurements

The changes in surface topography of the samples during the tests were monitored with the aid of a stylus profilometer with tip radius of 1µm and resolving power of 0.01µm. A cut-off length of L=0.8mm was selected for all the measurements according to ISO 4288 standard, so the total traversing length was 4.8 mm (0.4mm pre-travel+4mm evaluation length+0.4mm post-travel). A Gaussian filter was used in all measurements. Roughness parameters Ra, Rq, Rpk, Rvk, Rsm, Rk, Rsk following ISO 4287 standard, defined in Figure 3, were used to characterize the surfaces.

Ra is the mean height of the roughness profile, Rq is the root mean square of the roughness profile heights, Rsk (Skewness) is the third central moment of profile amplitude probability density function, measured over the assessment length used to measure the symmetry of the profile about the mean line, Rk (Kurtosis) is the fourth central moment of profile amplitude probability function, measured over the assessment length and describes the sharpness or flatness of the probability density of the profile, Rsm is the mean spacing between profile peaks at the mean line (see Gadelmawla et al.⁽⁶⁾ for details and definitions of the measured parameters). The Abbot Firestone curve or bearing area curve is defined as the percentage of solid material of the profile lying at a certain height which would result if the surface were abraded away down to a level plane; it is useful as an indicator of effective contact area at a specific height. Rpk and Rvk are defined as the height of triangles resulting from the intercept of a straight line projected through the axes of the Abbott Firestone curve.⁽⁷⁾ The peak height Rpk is defined as the height of the protruding peaks above the roughness core profile and the valley depth Rvk is defined as the depth of the profile valleys under the roughness core profile (see Figure 3).

Roughness values were measured before and during each hour of cavitation erosion tests. The values correspond to the average of 10 measurements performed on different directions on randomly areas of each GMAW-P samples.

$$R_a = \frac{1}{l} \int_0^l |y(x)| dx$$

$$R_q = \sqrt{\frac{1}{l} \int_0^l \{y(x)\}^2 dx}$$

$$R_k = \frac{1}{R_q^4} \int_{-\infty}^{\infty} y^4 p(y) dy$$

$$R_{sk} = \frac{1}{R_q^3} \int_{-\infty}^{\infty} y^3 p(y) dy$$

$$R_{sm} = \frac{1}{N} \sum_{i=1}^N Sm_i$$

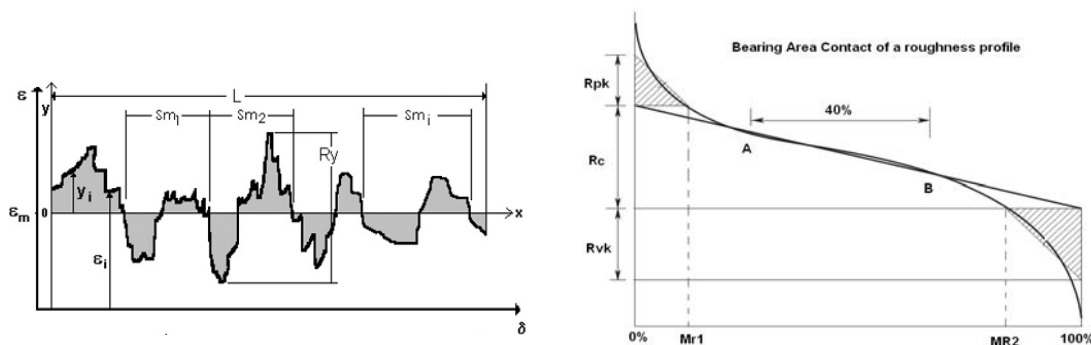


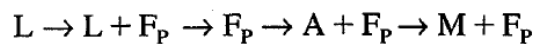
Figure3. Analytical definition of roughness parameters.

3 RESULTS AND DISCUSSION

3.1 Microstructure

Figure 4 shows the microstructure of 13Cr-4Ni steel and the welding coatings. In all cases, a martensitic microstructure with needle-like morphology is observed, although in the coatings a dendritic structure can also be seen.

The uncoated steel has an average hardness of 280 HV_{62.5}, 15% retained austenite and 4% delta ferrite.⁽⁸⁾ Regarding the microstructure of the coatings, the main difference between them is the mean size of the dendrites, which is related to the variations in heat input and consequently in the cooling rates. Pulsed current during welding causes a refinement of the microstructure which can be beneficial to improve mechanical and surface properties. In this case, the solidification path of welded martensitic stainless steel is described by the following sequence:



Where L: liquid, F_p: Delta Ferrite, A: austenite and M: martensite.^(9,10) This type of solidification indicates that some delta ferrite remains unchanged at room temperature, corresponding to the inter-dendritic regions shown in Figures 4b to 4d with white arrows. Therefore, the average dendritic size is lower in GMAW-P samples.

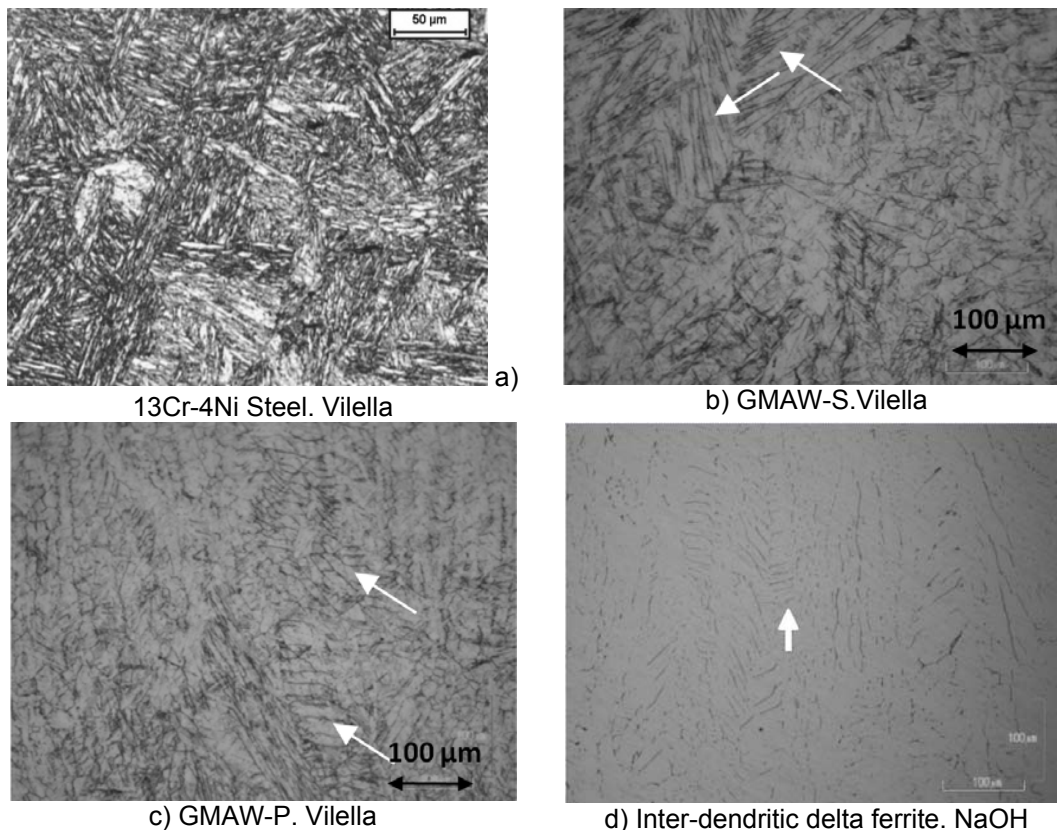


Figure 4. Microstructure of the coatings and 13Cr-4Ni steel.LOM.

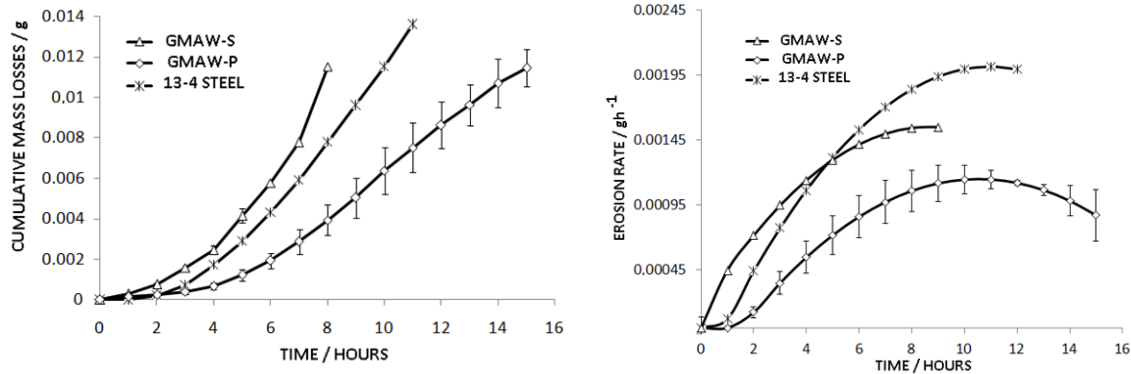
3.2 Cavitation Erosion Resistance

Figure 5a shows the variation of cumulative mass loss as a function of testing time for all the studied samples. It can be seen that pulsed coatings (GMAW-P) showed the best behavior of all the materials tested. For instance, after a reference testing time of 8 hours, the cumulative mass loss of GMAW-P coating samples was 3 and 2 times lower than that of reference materials GMAW-S and 13Cr-4Ni steel, respectively. The highest mass losses were reported by GMAW-S. The results indicate that repairing a worn turbine or a component with the GMAW-S procedure used in this work will reduce its wear resistance since the cavitation erosion is lower than that of 13Cr-4Ni steel (substrate).

Figure 5b shows the instantaneous erosion rate during the tests. The maximum erosion rate for the tested materials was reported by 13Cr-4Ni steel followed by GMAW-S. The steady erosion rate of the coatings was lower than that of the substrate in all cases. Another important information that can be extracted from Figure 5 is the time to reach the maximum erosion rate. For the coatings and the substrate this time is around 9 hours showing the importance of microstructure in cavitation erosion response. Besides the differences in incubation period (see next section for details), the steady state is mainly governed by the general microstructural aspects which are very similar (martensitic microstructures with delta ferrite in all cases).

With respect to the incubation stage, two calculation methods were used to estimate the incubation period of the samples (see Figure 6). Method A is described in the ASTM G32 standard and defines the incubation time as the intercept on the testing time axis of a straight line extension of the maximum-slope portion of the cumulative erosion-time curve. According to the results of this method, the longest incubation period was found in GMAW-P coatings (4.9 hours) followed by GMAW-S coatings (4.2 hours), while the 13Cr-4Ni steel exhibited the shortest one (4 hours). However, if a different criterion is used to calculate the incubation period (Method B) the results are in better agreement with the overall aspect of the cumulative mass loss curves, where GMAW-S clearly shows higher mass losses than 13Cr-4Ni steel. Method B is based on the simplest definition of incubation period, i.e. the period between the beginning of the test and the moment when the mass loss of the sample is no longer negligible. If method B is used, the measured values of incubation period represent a more realistic description of the behavior of the materials during cavitation erosion tests. In this work, it was assumed that mass losses higher than 10% of the maximum mass loss registered during the test cannot be considered negligible.

The differences in incubation period of the studied samples are related to the ability to deform plastically and the maximum mechanical resistance of the materials. Mechanical tests reported elsewhere^[11] showed that the tensile resistance and area reduction of GMAW-P coatings were 6% and 33% higher than those of the GMAW-S coatings, respectively. This result is significant because it has been shown that properties obtained in tensile testing can be good indicators of cavitation erosion resistance when comparing materials with similar microstructure.⁽¹²⁾ However, the response to cyclic loads should be taken into account to conclude about cavitation erosion from tensile testing of materials with different microstructures.⁽¹²⁾



a) Cumulative mass losses in cavitation erosion tests. b) Erosion rates in cavitation erosion tests.

Figure 5. Results from cavitation erosion tests.

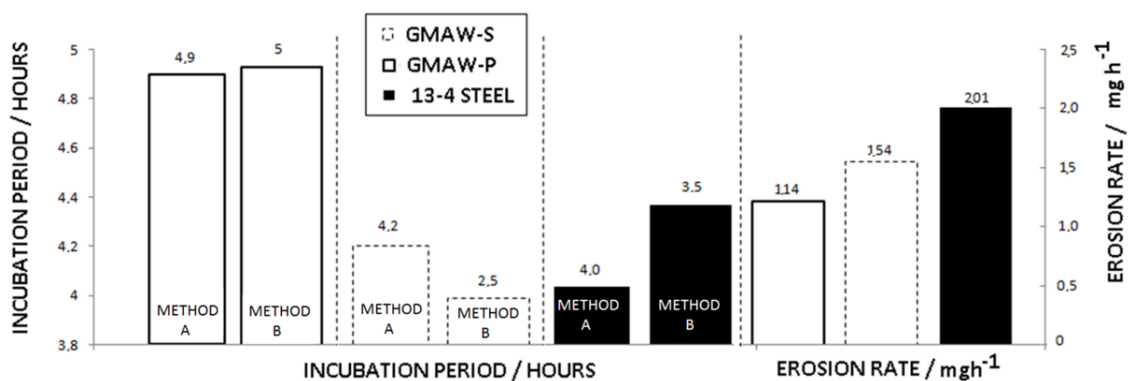


Figure 6. Incubation period and maximum erosion rate in cavitation erosion tests. Method A: According to ASTM standard Method B: Based on an offset of 10% of the maximum value of mass loss during the test.

3.3 Roughness Measurements During Cavitation Erosion Tests

Figure 7a shows the variation of R_a , R_q and $R_{sm}R_q^{-1}$ during cavitation erosion tests; Figure 7b shows the variation of R_{pk} and R_{vk} , Figure 7c show the variation of R_{sk} and Figure 7d show the variation of R_k and $R_a.R_q^{-1}$.

Frequently, the analysis of data from cumulative mass losses or erosion rate is not enough to identify different cavitation stages. However, if the evolution of surface roughness is taken as an indicator, several stages can be clearly identified as follows:

Region I, from 0h to 2h, is characterized by the greatest slope in $R_{sm}R_q^{-1}$ curve while no significant changes in R_a , R_q and mass loss were observed. The increase in R_{sk} reveals that the surfaces are changing in favor of displacing material from peaks instead of valleys. On the other hand, R_k did not change significantly during this stage.

Region II, from 2h to 6h, shows an increase in the erosion rate due to significant detachment of material from the surface. R_a and R_q curves start to separate from each other as a consequence of the higher sensibility of R_q to detect individual irregularities on the surface. Also, $R_{sm}R_q^{-1}$ presents a gradual decrease in slope until it reaches almost its minimum at the sixth hour. The formation of deep valleys is preferred over formation of high peaks (see Figure 7b), which makes R_{sk} values smaller. In addition to that, the behavior of $R_a.R_q^{-1}$ seems to be specular reflection of the R_k behavior.

In region III, from 6h to 15h, all roughness parameters remain stable and an approximately constant slope is observed in the cumulative mass loss curve. The results discussed above indicate that roughness measurements help identifying the wear mechanism acting during the incubation period, even before any substantial mass losses are registered. In particular, it can be said that after the sixth hour of testing the worn surface topography does not have a preferential texture in terms of valleys or peaks since R_k and R_{sk} parameters are very stable.

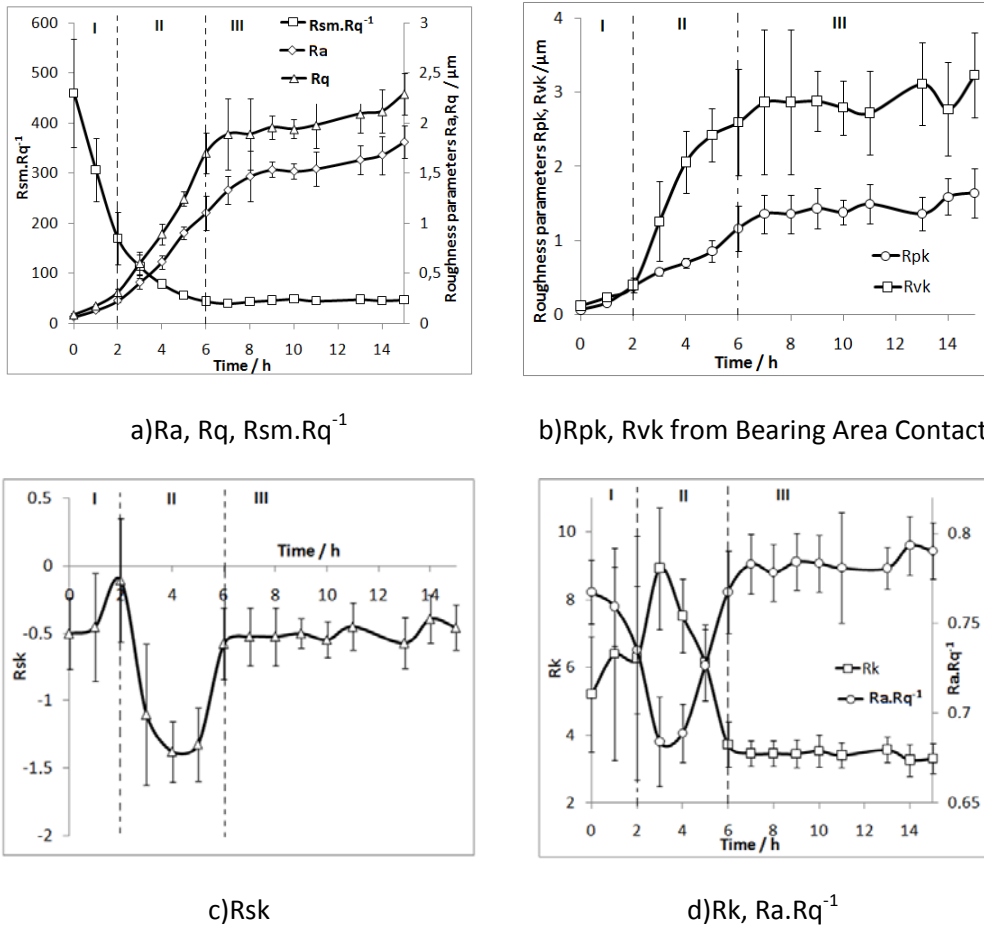
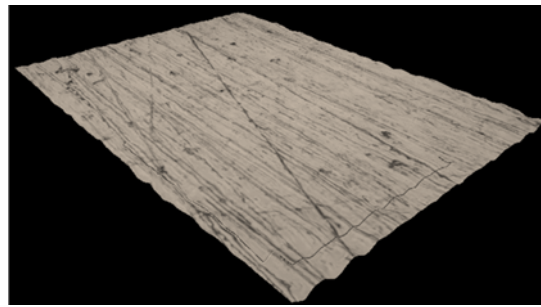


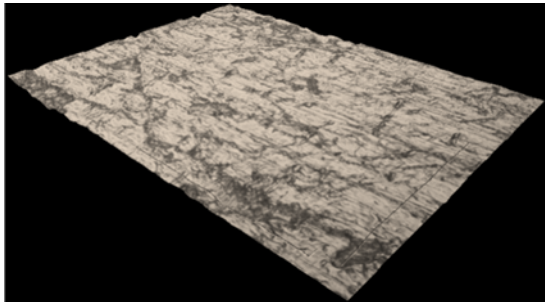
Figure 7. Variation of surface roughness parameters during cavitation erosion tests.

3.4 Analysis of Worn Surfaces

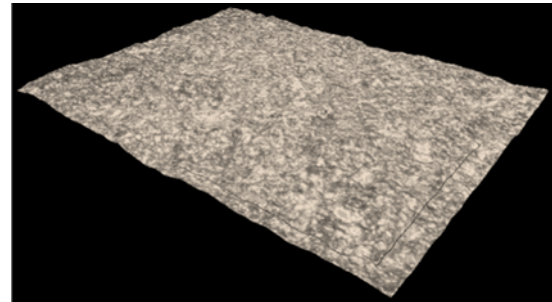
Figure 8 shows the aspect of the worn surfaces during the cavitation erosion tests. It can be seen that small pits appeared first at the valleys, and preferentially on or by the lines resulting from polishing procedures. Worn surfaces at the first, third and tenth hour of cavitation erosion test are shown.



a) First hour of testing GMAW-P



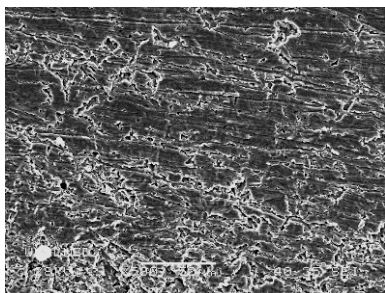
b) Third hour of testing GMAW-P



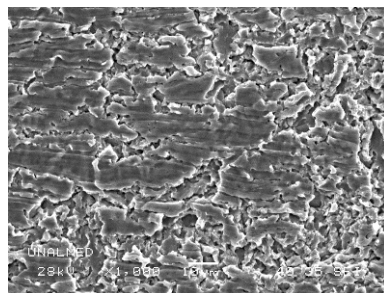
c) Tenth hour of testing GMAW-P

Figure 8. Typical aspect of worn surfaces at different stages of cavitation tests.

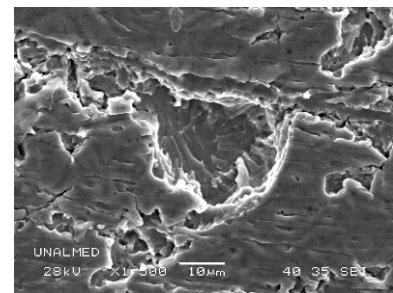
Figure 9 shows the worn surfaces of GMAW-P coatings after the cavitation erosion tests. Figure 9a shows a general image of the surface where the grinding lines can be observed. Figure 9b shows that the main removal mechanism is detachment of large particles as a consequence of coalescence of cracks propagating by surface fatigue. The detachment occurs preferentially from the valleys of surface roughness. Figure 9c shows a detail of striations on the worn surfaces. Those marks are typically found in surfaces submitted to cavitation erosion tests and are related to fatigue caused due to repetitive impact of shock waves on the surfaces due to the collapse of bubbles.⁽¹³⁾



a) 500X



b) 1000X



c) 1500X

Figure 9. Worn surfaces of GMAW-P after cavitation erosion test.

4 CONCLUSIONS

- The GMAW-P coatings showed the highest cavitation erosion resistance compared with GMAW-S and 13Cr-4Ni Steel.
- After a reference time of 8 hours of testing, the cumulative mass loss of GMAW-P coating samples (3.93mg) was 3 and 2 times lower than that of

reference materials GMAW-S (11.49mg) and 13Cr-4Ni steel (7.8mg), respectively.

- The incubation period (5h) of the GMAW-P coatings showed a considerable improvement of 33% and 50% compared with those of 13Cr-4Ni steel and GMAW-S respectively. The maximum erosion rate of GMAW-P coatings (1.14 mgh^{-1}) was lower than the 13Cr-4Ni substrate (2.01 mgh^{-1}) and GMAW-S coatings (1.54 mgh^{-1}). The roughness measurements helped to identify three different stages during the cavitation erosion test even when the measured mass losses were not significant.
- The worn surfaces showed striations typical of surface fatigue. The mass losses resulted mainly from valleys as shown by the evolution of roughness parameters detached by coalescence of cracks.

Acknowledgements

The authors thank to Dirección de Investigación (DIME) of Universidad Nacional de Colombia, Sede Medellín for their financial support provided by DIME project No. 20201008220.

REFERENCES

- 1 K.E. Easterling "Introduction to the Physical Metallurgy of Welding", Butterworths. Monographs in Materials, Butterworths & Co., London, 1983.
- 2 Kou, Sindo. Welding Metallurgy. Second Edition. Editorial WILEY INTERSCIENCE. United States of America. 2002.
- 3 Y.S. Kim, T.W. Eagar, Metal transfer in pulsed current gas metal arc welding, Weld. J. 72 (7) (1993) Pag 279–287.
- 4 P.K. Palani a, N. Murugan. Selection of parameters of pulsed current gas metal arc welding. Journal of Materials Processing Technology 172 (2006) 1–10 Review.
- 5 Y.S. Kim, T.W. Eagar. Analysis of metal transfer in gas metal arc Welding .Weld. J. 72 (7) (1993) Pag 269-278.
- 6 E.S Gadelmawla et al. Roughness parameters. Journal of Materials Processing Technology 123 (2002) Pag 133-145.
- 7 Tom R. Thomas. Rough Surfaces, 2ed. Imperial College Press, 1999, ISBN: 1860941001. Pag 144-146
- 8 Pacheco Gómez, Hernando. Transformaciones de fase causadas por un tratamiento térmico posterior a la soldadura en acero inoxidable martensítico ASTM grado CA6NM. Universidad Nacional de Colombia, Sede Medellín. 2008. Pag 44-63.
- 9 John C. Lippold, Damian J. Kotecki - Welding Metallurgy and Weldability of Stainless Steels Wiley .ISBN: 0471473790. 2005
- 10 R.J. Castro y J.J. de Cadenet. Metallurgy of stainless and heat resisting steels, Cambridge University Press. Pag 48-50.
- 11 J.D Escobar et al. Evaluación mecánica, tribológica y microestructural de soldaduras de acero inoxidable martensítico del tipo AWS A5.9 ER 410 NiMo. III CONFERENCIA INTERNACIONAL DE SOLDADURA Y UNIÓN DE MATERIALES ICWJM 2010.
- 12 Heathcock, et al. Cavitation erosion of stainless steel. Wear 81 (1982) Pag 311 – 327.
- 13 Turani Vaz, Cláudio. Avaliação da resistência à erosão por cavitação do metal de soldas produzidas com consumíveis tipo 13%Cr - 4%Ni - 0,4%Mo. Dissertação de Mestrado. Universidade Federal de Minas Gerais. 2004.